Electron Field-Emission in the ERL-Electron Source and the Projection Model

Vaibhav Kukreja
Department of Physics, Cornell University, Ithaca, New York, 14853
(Dated: December 16, 2005)

The electron source of the x-ray Energy Recovery Linac has to be operated with very high DC voltages to produce the small emittances that are sought. One limit to this voltage is electron field emission. We have tested two new electrodes with varied composition and surface preparation. In this report, we will present their emission activity and discuss two modifications in the traditional Fowler-Nordheim field emission model that may explain the large enhancement factors and the small emitting areas obtained from the emission behavior of our samples. In particular, we will introduce the model of superposed geometrical protrusions and a generalized model of n-emitters through the Fowler-Nordheim emission model. The 304 Stainless steel sample has shown exceptional results with very little emission activity up to fields of 27 MV/m, surpassing the performance all of the previously tested electrodes.

I. INTRODUCTION

The notion of pure metallic Fowler-Nordheim field emission, also known as cold electron emission, originated from the theory of electron field emission developed in 1920's. In this model, electrons are field emitted from one or two microscopic projections present on a broad-area cathode surface. These projections, also called microprotrusions, are quite sharp and lead to geometric enhancement of the local field at the projection site to a value that is 100 times greater than the value of nominally applied value (the field can be locally enhanced to value $\geq 10^9$ V/m [1]). Consequently, one observes field emission at fields at about 100 times less than the fields required for the classic field emission as proposed by Fowler and Nordheim [4].

Over the years, the projection model has lost its appeal to other models that involve the presence of insulating materials at the site of emission. One of the primary reasons for this is rooted in the lack of physical evidence for projections of sufficient sharpness to explain the low threshold fields observed for field emission. Even with the modern scanning electron microscopes, there has been little luck in finding such types of projections [4]. However, it turns out that it is possible to explain projections of such acute sharpness from the projection model itself. This is done via superposing a projection on a projection (see the Theory: The Projection Model section for a complete discussion of this).

Electron field emission behavior from board-area electrodes is very complex and not well understood. With large surface electrodes such as ours, the likelihood of multiple, rather one or two, sites of emission is very high. This is one of the many difficulties in applying Fowler-Nordheim model, which assumes presence of a single emitter, to understand emission from board-area electrodes. To put it more openly, our knowledge of electron field emission, especially from large area electrodes under the influence of high DC voltage, is remarkably small. Without a sound model of field emission, the fact remains that we do not have a well-defined criteria for choosing materials and surface processes that would guarantee a steady high voltage gap in DC electrons guns [2]. To get around this problem, we constructed a test

chamber that allows us to measure field emission from broad-area electrodes and evaluate this behavior in the framework of the Fowler-Nordheim model.

II. EXPERIMENTATION

The experimental chamber used in our recent studies is the same as in our earlier work (see [3] for a general description and [2] for more a detailed discussion). Therefore, we give a brief description of our experimental apparatus and methods. Below in figure 1 is a diagram of the chamber and other auxiliary components. The experimental chamber is built around a stainless steel six-way vacuum cross and the entire apparatus stands on a thermally insulated table. The ceramic insulator sits on top of the cathode and it is electrostatically shielded. Several different types of pumps are used to rid the chamber of contaminants and residual gases. The cathode is placed on a circular tube and it faces the anode held in position by an appropriate weight.

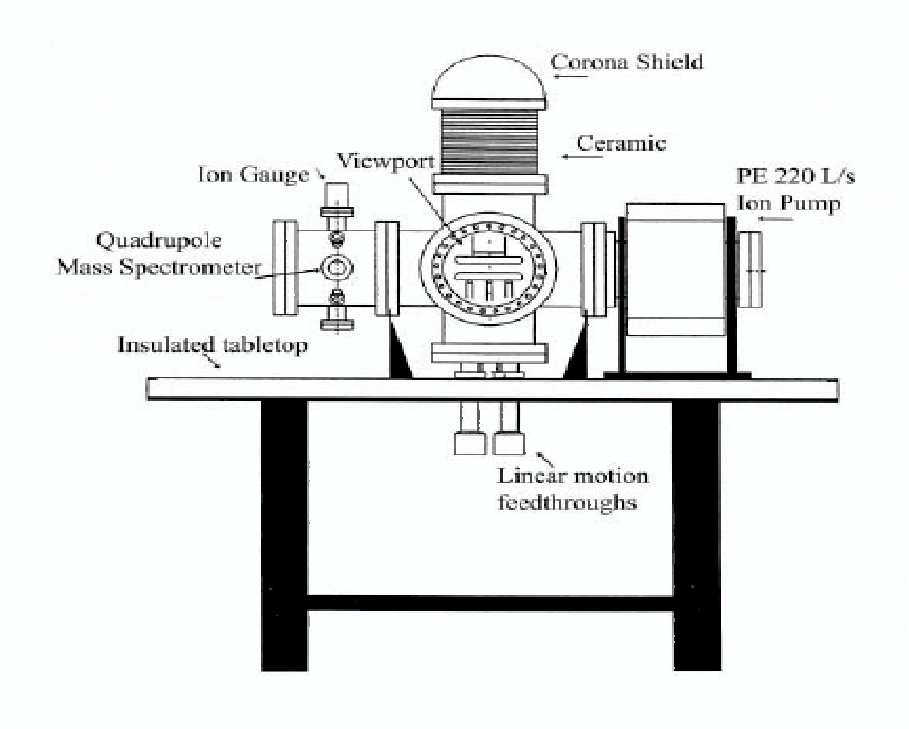

FIG. 1: A Schematic view of the electrode test chamber

All of the electrodes tested have identical surface area of 100 cm^2 and are shaped with a quasi-Rogowski profile. In all tested samples (both in our recent studies and earlier work), the anode was Ti4V6A1. This is a common Titanium alloy for structural applications with composition of 90% Ti, 6% Aluminum, and 4% Vanadium. The surface of the anode was prepared using a chemo-mechanical polishing technique. The anode electrode was first hand polished with diamond paste to a 6-9 μm surface finish. Then, the sample was polished with a solution of hydrogen peroxide and 0.05 μm colloidal Silica (SiO_2). The cathodes samples that we have just tested are 304 Stainless steel and 316 Stainless steel (abbreviated as SS#3 and 316LN† in the rest of the report). Both of these samples were polished at

Wilson Laboratory and received further surface coating treatment done by the Epion (see [3] for the details on the Epion process). Note that 316LN† is the same cathode sample as in [3], however that sample was *never* treated with any coating.

All samples were moved into and from the chamber in an open, dust-free environment. To lower the likelihood of contamination during the electrode changing, extra precautions were taken to cover the sample and the chamber from the open air. Furthermore, the chamber with the electrode was baked at 250 C to remove most of the remaining contaminants. The electrodes are tested in two phases. During the day (phase 1), current conditioning is applied to the sample. The measurements of prebreakdown current and power supply voltage are taken. After the day (phase 2), the electrode is quickly retested with the applied voltage increased in increments of 4 kV or 5 kV up to the maximum voltage reached in the days run. This allows us to get a smooth hysteresis curve of the field emission behavior. Again, the measurements of prebreakdown current and voltage are recorded. The prebreakdown or emissions currents are measured with a Keithley picoammeter.

III. RESULTS

We report measurements on two samples: SS#3 and 316LN† (*Epion coated*). As mentioned earlier, these two samples were prepared in the same way. After machining, the parts are sanded with a series of finer and finer silicon carbide abrasive papers to 600 grit. Then a suspension of diamond powder in oil is used to polish them further, starting with 9-micron diamond powder and working down in size to 1 micron. The polishing process takes 7-10 days of work to get a good Rogowski profile electrode. The SS# 3 was made of 304 Stainless steel, a different alloy from 316LN. 316LN is exceptionally hard, but polishes better. Both of the samples were sent to Epion for surface coating. The emission performance of the SS#3 and 316LN† sample is shown in figures 2 and 3 respectively. To see how the Epion coating would affect the electrode surface, we took before and after images of the treated 316LN sample using an interferometric light microscope (see figures 6-7 below). The dark brown regions are grooves or scratches (down into the material), while the white spots are dust specks or high spots. The height range from the darkest to lightest area is about 500 nm (a *very* rough estimate). The dramatic changes in the appearance of 316LN surface after treatment might explain the *unusual* amount of emission activity from this sample (see the Discussion section for more details), which we will discuss promptly.

As discussed in the beginning, the SS#3 is by far the best sample we have tested. With barely any field emission at *27 MV/m* (see figure 2) and signs of considerable processing while and after conditioning on day 1, we attempted to repeat this gap performance on day 2. However, unfortunate breakdowns in the high voltage cable halted this goal.[1] The next sample tested was the 316LN†, which in our earlier work (see [3] denoted there as just 316LN) reliably showed no signs of field emission up to 16 MV/m. The reliability of the high voltage gap is important to fulfill the requirement of operating the ERL electron gun at a field of 15 MV/m consistently with no signs of electron emission. However, after the Epion

[1] The breakdown in the cable occurred at a nominal voltage of 114 kV and at a field of 28.63 MV/m. After a lot of testing, we were able to match consistently (see figure 4) the emission curves (for SS#3 sample) before and after the cable fix up to a voltage of $\approx$ 100 kV, indicating that the breakdown in the cable was only occurring at voltages beyond this critical value.

coating, the sample was field emitting severely with a emission current of 50 nA at a minor nominal voltage of 5 kV and $\approx$ 8000 nA at 50 kV. Although these emission currents told us that the 316LN surface was significantly altered by the coating, we continued to put more voltage for any signs of processing. With currents reaching 105000 nA at 90 kV, this goal was clearly unfeasible (see figure 3). Note below are two tables containing the enhancements factors and emitting areas for all of the samples.

TABLE I: Enhancement Factors (β) and Emission Areas (A_e) while Current Conditioning

Electrode	Day	Gap (m)	$\phi(eV)$	Slope (A/V)	Intercept (A/V^2)	β	$A_e(m^2)$
316LN	1	0.00381	4.5	-33844	-11.058	305	2.9496E-17
316LN	2	0.00381	4.5	-35917	-11.165	288	2.5940E-17
316LN	3	0.005042	4.5	-38634	-12.565	354	1.1954E-18
316LN-R	1	0.004026	4.5	-20129	-13.939	542	1.3710E-20
CuBe	1	0.003922	4.65	-17563	-13.597	636	2.3303E-20
SS#5	1	0.004077	5	-30234	-12.027	428	2.6347E-18
SS#5	2	0.004077	5	-40996	-10.878	316	6.8214E-17
SS#5	3	0.004077	5	-32002	-12.233	405	1.8374E-18
SS#5	4	0.004077	5	-22916	-12.396	565	6.4611E-19
Ti#4	1	0.004813	4.33	-10591	-13.951	1163	3.6272E-21
Ti#4	2	0.004813	4.33	-12735	-15.012	967	4.5529E-22
SS#3	1	0.00403	4.5	-209162	-18.039	522	1.1766E-24
316LN†	1	0.00385	4.5	-666	-14.165	156629	8.9295E-26

TABLE II: Enhancement Factors (β) and Emission Areas (A_e) after Current Conditioning [a]

Electrode	Day	Gap (m)	$\phi(eV)$	Slope (A/V)	Intercept (A/V^2)	β	$A_e(m^2)$
316LN	1	0.00381	4.5	-46109	-9.6497	224	1.4013E-15
316LN	2	0.00381	4.5	-50851	-9.5329	203	2.2304E-15
316LN	3	0.005042	4.5	-76024	-8.5754	180	4.5204E-14
316Ln-R	1	0.004026	4.5	-27158	-12.865	402	2.9623E-19
CuBe∗	1	0.003922	4.65	-17563	-13.597	636	2.3303E-20
CuBe	1	0.003922	4.65	-13164	-13.716	848	9.9507E-21
SS#5	1	0.004077	5	-41498	-10.771	312	8.9455E-17
SS#5	2	0.004077	5	-39481	-11.085	328	3.9320E-17
Ti#4	2	0.004813	4.33	-33854	-12.776	364	5.5409E-19
SS#3	1	0.00403	4.5	-699765	-13.169	156	9.7689E-19
316LN†	1	0.00385	4.5	-236	-13.622	442878	3.9077E-26

[a]For a comparison, we have put Cube∗ in Table II to indicate the values from during the current conditioning.

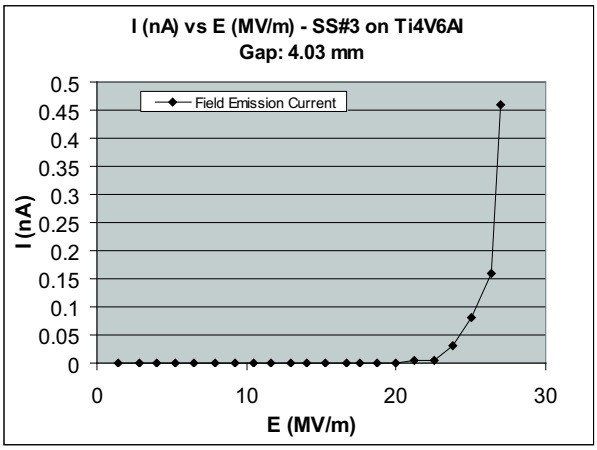

Figure 2: Emission behavior from the SS#3 stainless steel

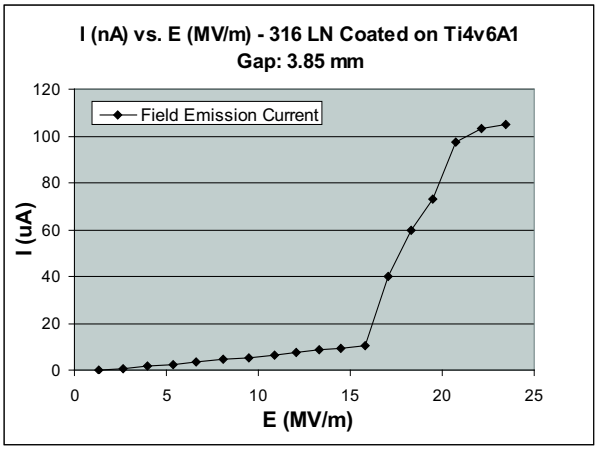

Figure 3: Emission behavior from the 316LN† stainless steel

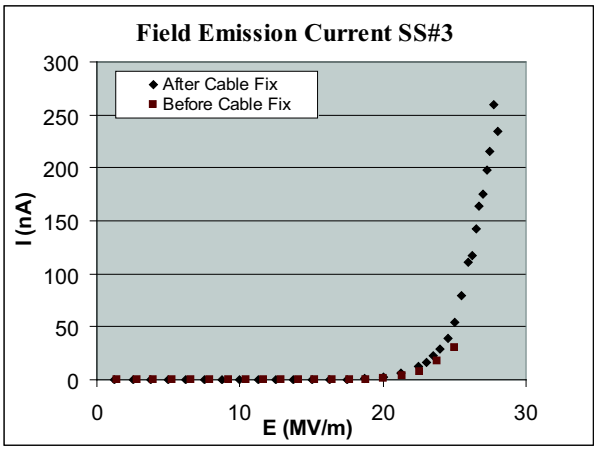

Figure 4: Emission behavior before and after the cable fix

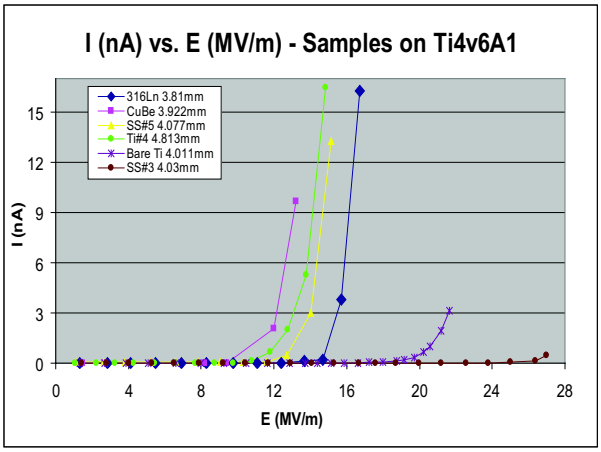

Figure 5: Collective Emission behavior from all samples

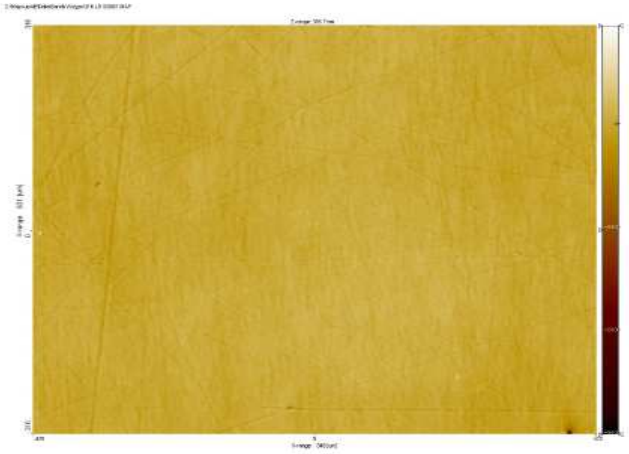

Figure 6: Surface Image of 316LN stainless steel before coating

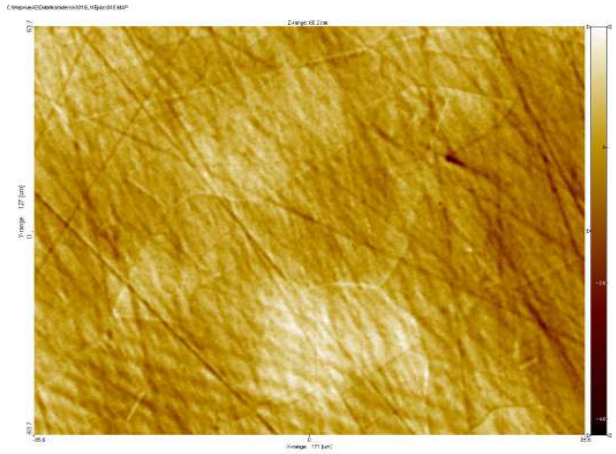

Figure 7: Surface Image of 316LN stainless steel after coating

IV. DISCUSSION

One thing that immediately stands out in the tables above is the enormous values of enhancements factors for the 316LN† electrode. The application of the Fowler-Nordheim

model to the emission current of this sample clearly fails and produces incorrect results. To provide a possible explanation for such enormous emission current, we will instead rely on qualitative evidence. This evidence is present in figures 6 and 7 above. One can see that the image before the coating displays a very clean, smooth surface only with scratch patterns from the surface finish. In comparison, the second (after coating) image shows the presence of grain-like structures, which we have never seen. We believe that these grains are the source of not just one or two potential emitters, but possibly of hundreds of emitters. The presence of dark brown layers in between the white layers may represent strips of cracks, and the entire strip might be field emitting. Such heavy field emission activity at low fields is something we have not seen in other samples coated by Epion, for example the SS#5 electrode (made of 304 stainless steel). However, it is interesting to note that SS#3 sample which has shown incomparable performance was also treated with the Epion process and yet it does not display any of the symptoms from the 316LN† sample. Again, this example shows the complexity involved in predicting the emission behavior from board-area electrodes.

V. THEORY: THE PROJECTION MODEL

As mentioned in the introduction, one of the puzzling concerns about the Fowler-Nordheim field emission model, also commonly called the Projection model, deals with the implausibility of projections of sufficient sharpness. Calculations have shown that the enhancement factor β for projections with simple geometry such as hemispheroids and cylinders with capped spheres is given by the ratio between the height of projection and the radius of tip [4]. The values observed for enhancement factors are in the range of 100-1000 [1] but the typical range is 100-200 [4]. So for the sake of our discussion, let us consider a enhancement factor of 100. Based on the ratio (as discussed above), a simple shape such as the hemispherically capped cylinder (denoted HCC) would need to have a height that is about hundred times taller than its radius. Through careful studies done involving particles with irregular geometries and mechanical damages on large area surface electrodes (see [4]), no direct evidence has been found for such pointed projections.

A group studying electron field emission lead by M. Jimenez (see [4]) proposed a model to attain high values of enhancement factors from structures that are less sharp. In their model, they first consider a HCC with appropriate sharpness to yield an enhancement factor β_1. In an area quite close to its tip, the projection surface look locally flat, with a uniform local field E_1. This field is β_1 times greater then the nominally applied field E_o. Then a second smaller HCC with an enhancement factor β_2 placed on this surface alone experiences a tip field E_2 enhanced over E_1 by a factor of β_2. Consequently, the total enhancement $\beta = E_2/E_o = \beta_1\beta_2$. This last result follows from the limit where the ratio of the sizes of the two HCCs goes to infinity. Using this model, Jimenez and his colleagues were successfully able to simulate enhancement factor of 100 using POISSON. Furthermore, they have observed geometrical defects that do indeed lead to an field enhancement factor of 100 in the manner described by their model (see [4] for a more detailed discussion).

However, the problem of explaining of field enhancement factors that are much greater than 100 is still present. Along with this, there is an issue concerning the values for emitting areas calculated from the Fowler-Nordheim result (given below).

$$log(I/V^2) = log\frac{1.54 \times 10^{-6} A_e \beta^2 10^{4.52\phi^{-0.5}}}{\phi d^2} - \frac{2.84 \times 10^9 d\phi^{1.5}}{\beta}\frac{1}{V} \qquad (1)$$

The typical range for emitting areas is $10^{-16} < A_e < 10^{-12}\ m^2$) [1]. One can see in Table I and II that most of our samples have values that are much smaller than the typical range. In reading the literature on field emission, we have found a generalized version of the Fowler-Nordheim result mentioned above. We think that this might improve the situation associated with high enhancement factors and small emitting areas. The appropriate result [1] (where there are n emitters distributed over the cathode surface, each with its own enhancement factor β_i and emitting area $(A_e)_i$, the total current I, and C_1 and C_2 are fundamental constants as discussed in [3]) is given by:

$$I = C_1(V/d)^2\Sigma(A_e)_i\beta_i^2 exp(-C_2 d/V\beta_i) \tag{2}$$

Although we have not directly applied this result to any of our measurements, we can already see a few difficulties that may encounter if we tried. The first of these concern our inability to know beforehand how many emitters are present on the cathode surface. Beyond that, we have no physical mechanism that allows to measure the average values of enhancement factors and emitting areas (if we were use this theory under the assumption that we have n identical emitters). Nevertheless, it is possible that in the near future we will able to make such types of measurements, and verify the Fowler-Nordheim result in the case of multiple emitters. [2]

VI. SUMMARY AND CONCLUSION

In figure 5 above, we have plotted the emission from all of our samples (except the 316LN† Epion coated). The cathode electrodes from our earlier work are 316 Stainless Steel, Beryllium Copper, 304 Stainless Steel, Ti4V6A1 (differently treated from the anode), and Bare Titanium (with same makeup as the Ti4V6A1 alloy), and are denoted as 316LN, CuBe, SS#5, Ti#4, and Ti#3 respectively. From our recent work, only the emission current of SS#3 is plotted. The SS#3 electrode has definitely outdid the performance most of our samples by at least 8 MV/m. We will be retesting this sample to establish a consistent, reproducible gap field with no electron emission while closely examining the effects of Epion processing on electrode surfaces. On the theoretical front, the model of superposed geometrical protrusions may be a promising approach to get at least a better understanding of the field enhancement factors from our cathode electrodes.

---

[1] R. V. Latham, High Voltage Vacuum Insulation Academic Press, London, 1995.

[2] C. K. Sinclair et al., Dramatic Reduction of DC Field Emission From Large Area Electrodes By Plasma-Source Ion Implantation, Thomas Jefferson National Accelerator Facility, 2001.

[3] V. Kukreja, Field-Emission Properties in the ERL-Electron Source, Laboratory for Elementary-Particle Physics (REU), Summer 2005.

[2] Latham discusses in chapter 4 that a lot of work in this area has been done via computer simulation studies. What is generally found is that prebreakdown current are dominated by a collection of high-β emitters and their enhancement factor and emitting area appropriately appear in the Fowler-Nordheim plot.

[4] M Jimenez et al., Electron Field Emission from large-area cathodes: evidence for the projection model, J. Phys. D: Appl. Phys. 27, 1994.